JACS
JOURNAL OF THE AMERICAN CHEMICAL SOCIETY

Communication

pubs.acs.org/JACS

A Sustainable Template for Mesoporous Zeolite Synthesis

Robin J. White,*[,†,§] Anna Fischer,[‡] Caren Goebel,[‡] and Arne Thomas*[,†]

[†]Technische Universität Berlin, Department of Chemistry, BA2, Hardenbergstraße 40, 10623 Berlin, Germany

[‡]Technische Universität Berlin, Department of Chemistry, TK01, Straße des 17. Juni 135, 10623 Berlin, Germany

Supporting Information

ABSTRACT: A generalized synthesis of high-quality, mesoporous zeolite (e.g., MFI-type) nanocrystals is presented, based on a biomass-derived, monolithic N-doped carbonaceous template. As an example, ZSM-5 single crystals with desirable large-diameter (12−16 nm) intracrystalline mesopores are synthesized. The platform provides scope to optimize template dimensions and chemistry for the synthesis of a range of micro-/mesoporous crystalline zeolites in a cost-effective and highly flexible manner.

Zeolites are well-known crystalline molecular sieves, presenting uniform micropores of high internal surface area and, as a result of crystalline aluminosilicate chemistry, high Lewis/Brønsted acidity.[1] The molecular-sized sieves provide shape and size selectivity, exploited in catalysis, adsorbents development, and other emerging topics (e.g., CO_2 capture).[1,2] As a standard premise, the uniform porosity arises from the use of small organic molecular templates (e.g., tetrapropylammonium hydroxide, TPAOH) to generate ordered crystalline microporous phases.[3] The resulting crystal is composed of small channels (e.g., diameter (D) ≈ 0.8 nm) and cavities (e.g., D ≈ 0.3−1.5 nm), particularly suitable for traditional petrochemical catalysis (e.g., aromatic alkylations or isomerizations).[4] However, this highly defined microporosity can also be disadvantageous, particularly if mass transfer kinetics of bulkier molecules/reagents/products are considered.[5] Mesopores (D ≈ 2−50 nm) are considered as the critical size domain for mass transport/diffusion (e.g., in heterogeneous catalysis). Thus, there has been recent interest in the synthesis of zeolites featuring mesoporosity, in order to enhance reagent and product diffusion to and from catalytically active zeolite wall sites.[5−7] This material property will become increasingly important given the complex streams of future bio-refineries or alternative industrial schemes (e.g., the Methanol Economy).[8]

Hence, due to the potential application benefits of mesoporous zeolites, the development of simple, scalable synthetic methods is an important challenge. To minimize diffusion problems, efforts have explored the synthesis of zeolites with controlled particle morphology and porosity.[7,9] Other approaches have relied on steaming, leaching, chemical treatment, or increased molecular cation sizes to introduce varying degrees of mesoporosity.[10] Although generally successful in terms of improved diffusion, a reduction in pore-wall crystallinity is often observed, resulting in reduced catalytic activity.[11] One approach to overcome these limitations is to decrease the zeolite crystal size to the nanometer scale, consequently increasing external surface area while reducing the diffusion path length.[12] Alternatively, provided the mesopores are suitably sized (e.g., D > 5 nm), mesoporosity and hierarchical porosity can be introduced within the zeolite crystal/crystal assemblies.[13] In this context, endo- and exo-templating commonly associated with the synthesis of ordered mesoporous materials (e.g., silica, carbons) have received much attention in zeolite synthesis.[10,14] It is important to note that soft block-copolymer (i.e., micelle-forming) templates employed in amorphous mesoporous silica synthesis (e.g., SBA-15) are generally inappropriate for large mesopore generation due to high zeolite crystallization temperatures. While a variety of hard templates have been used, many do not introduce mesopores of D > 5 nm or offer scope for pore tailoring in unison with necessary pore-wall crystallinity.[15] It should be stated that, for most applications, notably catalysis, the presence of non-ordered mesoporosity is more than sufficient, as similar or better molecular transport pathways can be generated as compared with ordered mesoporosity.[16]

In terms of design, sacrificial hard templates of tunable dimensions/morphology, removable (e.g., via calcination) with the molecular micropore template, would be an appropriate solution to the aforementioned problems. Jacobsen et al. reported on the use of carbon black (CB, e.g., BP-2000 pearls) as a mesopore template.[6a,17] Impregnation with ZSM-5 precursor solutions followed by hydrothermal treatment and template removal produced broad intracrystalline mesopores in the zeolite crystal. Similar approaches have been reported employing carbon aerogels and monoliths.[18] Other porous carbons (e.g., 3DOM),[15,19] carbon nanoparticles,[20] and carbon nanotubes (CNTs)[21] have also been investigated. However, these approaches either are expensive (e.g., CNTs), are limited in terms of template sizes and surface chemistry, or suffer from poor crystallization control/aluminum incorporation, necessary to ensure catalytic activity and avoid the synthesis of nanosized, non-mesoporous zeolite crystals.

A variety of high surface area functional carbons synthesized from sugar-based biomass have recently been reported and appear to fulfill the aforementioned hard-template criteria.[22] For example, the hydrothermal carbonization of glucose in the presence of ovalbumin (a N-rich glycoprotein) yields high-volume, hierarchically porous, N-doped carbonaceous monoliths (NDCs).[23] The carbon network forms via the Maillard-type chemistry of glucose and protein amine groups, along with sugar dehydration to (hydroxymethyl)furfural and co-condensation/phase separation/network formation. The result is a hyper-

Received: November 13, 2013
Published: January 7, 2014

   dx.doi.org/10.1021/ja411586h | J. Am. Chem. Soc. 2014, 136, 2715−2718

Scheme 1. A Generalized Synthesis of Mesoporous Zeolites (e.g., ZSM-5)[a]

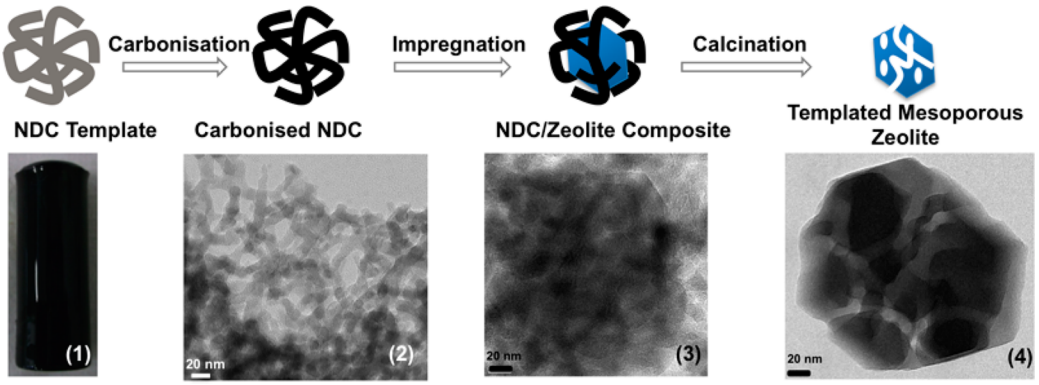

[a] Based on (1) and (2) biomass-derived NDC monolithic templates, followed by (3) NDC/(TPAOH)-zeolite preparation via impregnation and hydrothermal treatment, and (4) template removal via calcination to produce the templated mesoporous zeolite.

branched, highly porous carbonaceous monolith with relatively uniform branch widths (~14±2 nm), joining at thicker branch node points (>20 nm; Scheme 1 and Figure 1S). From a morphology point of view, the successful replication of such NDC structures into a solid inorganic phase (e.g., a zeolite) would generate fully interconnected large-*D* mesopores in the templated material. Furthermore, texture, dimensions, and chemistry (e.g., C and N condensation) of the NDC can be directed via precursor ratio, solvent volume, and postsynthesis thermal annealing, thus offering the flexibility required for a general approach.

As a demonstrative example, an NDC monolith[23] was used as a hard template in the synthesis of a model MFI zeolite (i.e., ZSM-5, Scheme 1). Prior to zeolite synthesis, the NDC was thermally treated at 550°C under N_2 to provide extra dimensional stability and reduce the possibility of capillary force-induced structural collapse as a result of aqueous solution impregnation (Scheme 1, (2)). The NDC monolith was evacuated under vacuum, followed by addition of ZSM-5 precursors (molar ratio H_2O/Al-$(OC_4H_9)_3$/Si$(OC_2H_5)_4$/TPAOH = 30.5:0.017:1.0:0.17) until saturation of the template (~3.7−4.0 mL). The impregnated monolith was then hydrothermally treated (160°C/72 h), followed by TPAOH/NDC removal by calcination to yield a white powder, termed Meso-ZSM-5 (Scheme 1, (3) and (4)). The intermediate material (i.e., after hydrothermal treatment/before calcination) is denoted as NDC/(TPAOH)-ZSM-5.

Powder XRD analysis of Meso-ZSM-5 reveals a typical diffraction pattern for well-crystallized (MFI) ZSM-5, in good agreement with the diffraction pattern of nontemplated ZSM-5 and literature/database values (Figure 1).[24] The formation of other crystalline phases was not observed. It is important to note that Meso-ZSM-5 crystallite size appears a little smaller than the control ZSM-5, as indicated by marginal line broadening. The corresponding XRD pattern for NDC/(TPAOH)-ZSM-5 presents the appropriate diffraction for (TPAOH)-ZSM-5,[24] with a broad amorphous feature of the NDC template ($2\theta \approx 24°$), demonstrating the ZSM-5 phase is formed during the hydrothermal synthesis. N_2 sorption analysis of Meso-ZSM-5 produces a type-IV/H3 reversible isotherm, distinct from the type-I profile of ZSM-5 (Figure 2), demonstrating mesoporosity is introduced as a result of NDC template use. In terms of surface area (Table 2S), Meso-ZSM-5 presents a larger S_{BET} = 330 m^2/g compared to the control ZSM-5 (S_{BET} = 250 m^2/g), the result of relative crystal size reduction (i.e., from >0.5 μm to <250 nm, Figure 2S). Micropore diameters in both cases were typical for

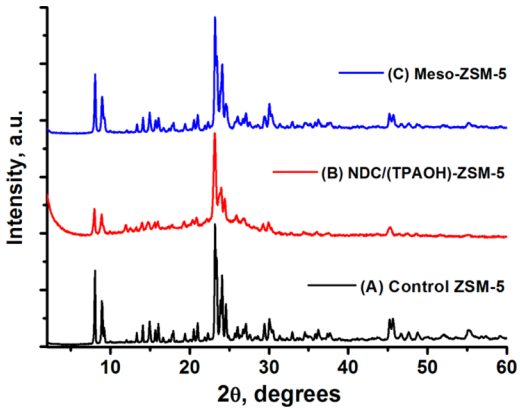

Figure 1. Wide-angle X-ray diffraction patterns for (A) control ZSM-5, (B) as-synthesized NDC/(TPAOH)-ZSM-5, and (C) Meso-ZSM-5.

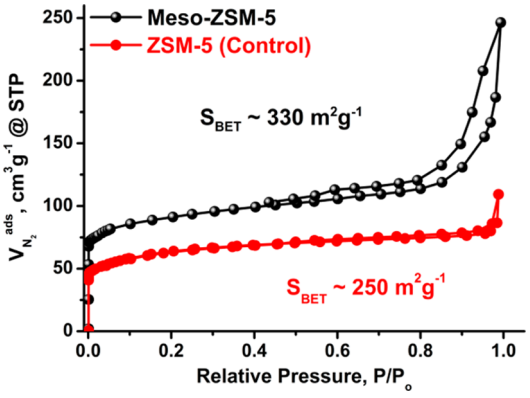

Figure 2. N_2 sorption isotherms for the control ZSM-5 and NDC-templated Meso-ZSM-5.

MFI-type ZSM-5 (i.e., 0.6 nm).[24] Micropore volume was ~0.13 cm^3/g for the control ZSM-5, not significantly altered as a result of hard templating ($V_{micro}^{(Meso\text{-}ZSM\text{-}5)}$ = 0.13 cm^3/g). Pore size analysis for Meso-ZSM-5 depicts a relatively broad distribution and porosity generation across the whole mesoporous range (Figure 3S). Rather defined pore diameters are observed with maxima of 10−20 nm. Considering the relatively uniform NDC branch diameters of ~12−16 nm, this indicates successful replication of the structure into the ZSM-5 crystal to generate mesopores. Such structuring is notably missing from the corresponding analysis

dx.doi.org/10.1021/ja411586h | J. Am. Chem. Soc. 2014, 136, 2715−2718

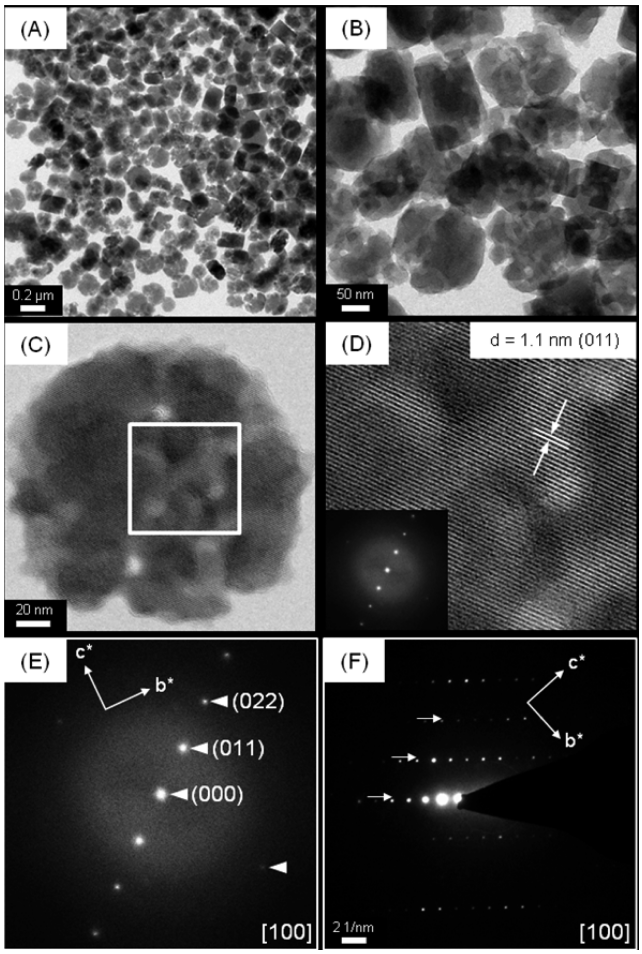

Figure 3. TEM images of (A,B) templated Meso-ZSM-5; (C) a single particle; (D) detail of the single particle in (C) with corresponding FFT (inset); (E) FFT of (D) with calculated Miller indices; and (F) SAED of Meso-ZSM-5 showing the monoclinic and pseudohexagonal symmetry with indexed *d*-values (projection [100]).

for the control ZSM-5. With regard to V_{meso}, this was calculated as 0.13 cm^3/g for Meso-ZSM-5, resulting in a promising 50:50 (micro/meso) volume ratio, with V_{total} = 0.30 cm^3/g.

TEM images of NDC/(TPAOH)-ZSM-5 indicate the confined formation of ZSM-5 crystals around the hyperbranched NDC template structure (Scheme 1, (3); Figure 4S). The confined ZSM-5 crystals are relatively uniform in size (≤200 nm), with higher magnification images indicating the zeolite crystal lattice planes within the porous carbon scaffold. TEM images of Meso-ZSM-5 demonstrate successful removal of the NDC template by calcination (Figure 3). Local energy-dispersive X-ray spectroscopy performed on single crystals gives a Si/Al ratio of 38.4 (0.63 at.% Al), indicating near-total incorporation of precursor Al into the final material (Figure 5S). Low-magnification TEM images reveal a relatively uniform particle size (~190±15 nm), with a variety of hexagonal particle shapes almost identical to those entrapped within the NDC template (Figure 3A,B). TEM images of a typical particle illustrate the clear mesoporous structuring in the ZSM-5 crystal. The branched and tortuous porosity, appearing relatively regular in diameter and extending through the entire crystal, is reflective of the NDC structure (i.e., branched cylindrical mesopores of *D* = 12−16 nm; Figures 3B−D and 6S). Comparison of the porous structure with the NDC template structure at the same length scale demonstrates successful template replication. This observation is in good agreement with the pore size distribution derived from N_2 sorption analysis.

Higher resolution TEM analysis reveals well-defined lattice fringes throughout, demonstrating the high crystallinity of Meso-ZSM-5. The measured interfringe distance of ~1.1 nm determined by fast Fourier transformation (FFT) corresponds to the expected *d*-value between (011) planes of MFI-type zeolites (Figure 3D,E). The selected area electron diffraction (SAED) of a typical Meso-ZSM-5 particle (along the [100] zone axis) confirms that Meso-ZSM-5 particles are single crystals (Figure 3F). Although ZSM-5 crystallizes in the monoclinic crystal system (i.e., $P12_1/n1$), a hexagonal morphology is observed for Meso-ZSM-5 particles (Figures 3E,F and 7S; Scheme 1, (4)), explained by the existence of an external pseudohexagonal crystal structure along with an internal monoclinic structure (as indicated by powder XRD and SAED analysis). In summary, these are significant findings demonstrating that the reported synthesis produces MFI-type zeolite particles with both promising micro-/mesoporosity and the material crystallinity required for catalytic applications. In terms of templating, the NDC branch dimensions should be easily manipulated (e.g., via precursor concentration, solvent volume, reaction time, etc.) to direct mesopore dimensions in the templated zeolite product. Furthermore, we speculate that the N-doped surface chemistry of the template may assist favorable interactions between the template surface and the zeolite precursors (e.g., silicic acid or (alumino)silicates) during network condensation/crystallization, enabling control of both crystallinity and mesoporosity. The N-doped surface chemistry/hydrophobicity of the NDC template can be tailored independently of the zeolite synthesis via carbonization at a desired temperature or by chemical modification (e.g., quaternization). Therefore, NDC templates can potentially be considered as a heterogenization of an "ammonium" template for mesopore generation.

From a process point of view, the presented mesoporous zeolite synthesis combines the benefits of a sustainable hard carbon template with space-confined synthesis, and should be extendable to a wide range of zeolite types. Given the 3D nature of the NDC template, impregnation could lead to intracrystalline mesoporous zeolite monoliths, provided precursor solution and template surface chemistry are optimized, potentially avoiding problems associated with industrial zeolite catalyst preparation (i.e., extrusion, inorganic binder use, pore blocking, and active species dilution). Considering the presented template is derived from sugar and egg protein precursors, it is anticipated, given the simple template synthesis/economies of scale, that NDC (or other sustainable carbons) will be more economically attractive industrially than previously reported templates (e.g., CNT ≥$13,800/kg; carbon nanofibers $3400/kg; CB pearls $8300/kg, NDC $1030/kg; see Supporting Information).[25]

In conclusion, a sugar/protein-derived monolithic NDC template provides the environment for the confined synthesis of relatively small single-crystal ZSM-5 particles (≤200 nm) featuring large-diameter (12−16 nm) mesoporosity, a result of replication of the branched NDC template structure. It is a viable approach to synthesize high-quality mesoporous MFI-type zeolite crystals with intracrystalline mesoporosity (and good Al incorporation). This approach provides scope to optimize NDC template dimensions and chemistry for the synthesis of different zeolites (e.g., crystal structures and sizes) in the form of nanoparticles and, potentially, monoliths. The impact and

dx.doi.org/10.1021/ja411586h | *J. Am. Chem. Soc.* 2014, 136, 2715−2718

necessity of an active N-doped surface chemistry for successful templating and mesopore/crystallinity generation are currently under investigation. Determination of the applicability of Meso-ZSM-5 as a heterogeneous catalyst is also envisioned. Moreover, the generated mesoporous domains are of a size that secondary catalytic species (e.g., Pt nanoparticles) could be introduced, making the material promising for highly efficient cascade, consecutive, or bifunctional catalytic applications.[26] This report represents a potential deviation from the classical confined-space templating approach, opening a platform for surface-active (e.g., N-doped carbon) hard templating, enabling the generation of desirable microporosity/interconnected mesoporosity and zeolite crystallinity using a simple, cost-effective, sustainable template.

■ ASSOCIATED CONTENT

Supporting Information

Experimental details and characterization data. This material is available free of charge via the Internet at http://pubs.acs.org.

■ AUTHOR INFORMATION

Corresponding Author

robin.white666@googlemail.com; arne.thomas@tu-berlin.de

Present Address

[§]Institute for Advanced Sustainability Studies e.V., Berlinerstr. 130, D-14467 Potsdam, Germany

Notes

The authors declare no competing financial interest.

■ ACKNOWLEDGMENTS

This work is funded by the Unifying Concepts in Catalysis Excellence Cluster. We thank C. Eichenauer for N_2 sorption analysis and M. Unterweger for XRD measurements.

■ REFERENCES

(1) (a) Venuto, P. B. *Microporous Mater.* **1994**, *2*, 297. (b) Corma, A. *Chem. Rev.* **1995**, *95*, 559. (b) Arends, I. W. C. E.; Sheldon, R. A.; Wallau, M.; Schuchardt, U. *Angew. Chem., Int. Ed.* **1997**, *36*, 1144. (c) Davis, M. E. *Nature* **2002**, *417*, 813. (d) Kresge, C. T.; Roth, W. J. *Chem. Soc. Rev.* **2013**, *42*, 3663.

(2) (a) Walton, K. S.; Abney, M. B.; LeVan, M. D. *Microporous Mesoporous Mater.* **2006**, *91*, 78. (b) Morris, R. E.; Wheatley, P. S. *Angew. Chem., Int. Ed.* **2008**, *47*, 4966. (c) Siriwardane, R. V.; Shen, M. S.; Fisher, E. P. *Energy Fuels* **2005**, *19*, 1153. (d) Harlick, P.; Tezel, F. H. *Microporous Mesoporous Mater.* **2004**, *76*, 71.

(3) (a) Morris, R. E.; Weigel, S. J. *Chem. Soc. Rev.* **1997**, *26*, 309. (b) Cundy, C. S.; Cox, P. A. *Chem. Rev.* **2003**, *103*, 663. (c) Davis, M. E. *Chem. Mater.* **2014**, *26*, 239.

(4) (a) Guisnet, M.; Gnep, M. S.; Morin, S. *Microporous Mesoporous Mater.* **2000**, *35*, 47. (b) Moliner, M.; González, J.; Portilla, M. T.; Willhammar, T.; Rey, F.; Llopis, F. J.; Zou, X.; Corma, A. *J. Am. Chem. Soc.* **2011**, *133*, 9497. (c) Qin, Z.; Lakiss, L.; Gilson, J. P.; Thomas, K.; Goupil, J. M.; Fernandez, C.; Valtchev, V. *Chem. Mater.* **2013**, *25*, 2759.

(5) (a) Corma, A. *Chem. Rev.* **1997**, *97*, 2373. (b) Kärger, J.; Valiullin, R. *Chem. Soc. Rev.* **2013**, *42*, 4172.

(6) (a) Madsen, C.; Jacobsen, C. J. H. *Chem. Commun.* **1999**, 673. (b) Schmidt, I.; Krogh, A.; Wienberg, K.; Carlsson, A.; Brorson, M.; Jacobsen, C. J. H. *Chem. Commun.* **2000**, 2157.

(7) van Donk, S.; Janssen, A. H.; Bitter, J. H.; de Jong, K. P. *Catal. Rev.* **2003**, *45*, 297.

(8) (a) Karinen, R.; Vilonen, K.; Niemelä, M. *ChemSusChem* **2011**, *4*, 1002. (b) Corma, A.; De La Torre, O.; Renz, M. *Energy Environ. Sci.* **2012**, *5*, 6328. (c) Zhao, C.; Brück, T.; Lercher, J. A. *Green Chem.* **2013**, *15*, 1720. (d) Huang, Y. B.; Fu, Y. *Green Chem.* **2013**, *15*, 1095. (e) Ilias, S.; Bhan, A. *ACS Catal.* **2013**, *3*, 18.

(9) (a) Smith, J. V. *Chem. Rev.* **1988**, *88*, 149. (b) van Donk, S.; Broersma, A.; Gijzeman, O. L. J.; van Bokhoven, J. A.; Bitter, J. H.; de Jong, K. P. J. *J. Catal.* **2001**, *204*, 272. (c) Tosheva, L.; Valtchev, V. P. *Chem. Mater.* **2005**, *17*, 2494. (d) Möller, K.; Bein, T. *Chem. Soc. Rev.* **2013**, *42*, 3689.

(10) Egeblad, K.; Christensen, C. H.; Kustova, M.; Christensen, C. H. *Chem. Mater.* **2008**, *20*, 946.

(11) (a) Zhou, J.; Hua, Z. L.; Shi, J. L.; He, Q. J.; Guo, L. M.; Ruan, M. L. *Chem.—Eur. J.* **2009**, *15*, 12949. (b) Wu, L.; Degirmenci, V.; Magusin, P. C. M. M.; Szyja, B. M.; Hensen, E. J. M. *Chem. Commun.* **2012**, *48*, 9492.

(12) (a) Möller, K.; Yilmaz, B.; Mueller, U.; Bein, T. *Chem. Mater.* **2011**, *23*, 4301. (b) Ng, E. P.; Chateigner, D.; Bein, T.; Valtchev, V.; Mintova, S. *Science* **2012**, *335*, 70. (b) Mintova, S.; Gilson, J. P.; Valtchev, V. *Nanoscale* **2013**, *5*, 6693.

(13) (a) Carr, C. S.; Kaskel, S.; Shantz, D. F. *Chem. Mater.* **2004**, *16*, 3139. (b) Möller, K.; Yilmaz, B.; Müller, U.; Bein, T. *Chem.—Eur. J.* **2012**, *18*, 7671. (c) Liu, F.; Willhammar, T.; Wang, L.; Zhu, L.; Sun, Q.; Meng, X.; Carrillo-Cabrera, W.; Zou, X.; Xiao, F. S. *J. Am. Chem. Soc.* **2012**, *134*, 4557. (d) Wang, X.; Li, Y.; Luo, C.; Liu, J.; Chen, B. *RSC Adv.* **2013**, *3*, 6295. (e) Yin, C.; Tian, D.; Xu, M.; Wei, Y.; Bao, X.; Chen, Y.; Wang, F. *J. Colloid Interface Sci.* **2013**, *397*, 108.

(14) (a) Schmidt, I.; Madsen, C.; Jacobsen, C. J. H. *Inorg. Chem.* **2000**, *39*, 2279. (b) Stein, A. *Adv. Mater.* **2003**, *15*, 763. (c) Schüth, F. *Angew. Chem., Int. Ed.* **2003**, *42*, 3604.

(15) (a) Sakthivel, A.; Huang, S. J.; Chen, W. H.; Lan, Z. H.; Chen, K. H.; Kim, T. W.; Ryoo, R.; Chiang, A. S. T.; Liu, S. B. *Chem. Mater.* **2004**, *16*, 3168. (b) Yang, Z. X.; Xia, Y. D.; Mokaya, R. *Adv. Mater.* **2004**, *16*, 727. (c) Fang, Y. M.; Hu, H. Q. *J. Am. Chem. Soc.* **2006**, *128*, 10636.

(16) Rolison, D. R. *Science* **2003**, *299*, 1698.

(17) (a) Jacobsen, C. J. H.; Madsen, C.; Houzvicka, J.; Schmidt, I.; Carlsson, A. *J. Am. Chem. Soc.* **2000**, *122*, 7116. (b) Janssen, A. H.; Schmidt, I.; Jacobsen, C. J. H.; Koster, A. J.; de Jong, K. P. *Microporous Mesoporous Mater.* **2003**, *65*, 59.

(18) (a) Holland, B. T.; Abrams, L.; Stein, A. *J. Am. Chem. Soc.* **1999**, *121*, 4308. (b) Christensen, C. H.; Johannsen, K.; Schmidt, I.; Christensen, C. H. J. *J. Am. Chem. Soc.* **2003**, *125*, 13370. (c) Tao, Y. S.; Kanoh, H.; Kaneko, K. *J. Am. Chem. Soc.* **2003**, *125*, 6044. (d) Li, W. C.; Lu, A. H.; Palkovits, R.; Schmidt, W.; Spliethoff, B.; Schüth, F. *J. Am. Chem. Soc.* **2005**, *127*, 12595.

(19) Fan, W.; Snyder, M. A.; Kumar, S.; Yoo, W. C.; McCormick, A. V.; Penn, R. L.; Stein, A.; Tsapatsis, M. *Nat. Mater.* **2008**, *7*, 984.

(20) Ok, D. Y.; Jiang, N.; Prasetyanto, E. A.; Jin, H.; Park, S. E. *Microporous Mesoporous Mater.* **2011**, *141*, 2.

(21) Schmidt, I.; Boisen, A.; Gustavsson, E.; Ståhl, K.; Pehrson, S.; Dahl, S.; Carlsson, A.; Jacobsen, C. J. H. *Chem. Mater.* **2001**, *13*, 4416.

(22) (a) White, R. J.; Antonietti, M.; Titirici, M. M. *J. Mater. Chem.* **2009**, *19*, 8645. (b) Wohlgemuth, S. A.; White, R. J.; Willinger, M. G.; Titirici, M. M.; Antonietti, M. *Green Chem.* **2012**, *14*, 1515. (c) Brun, N.; Wohlgemuth, S. A.; Osiceanu, P.; Titirici, M. M. *Green Chem.* **2013**, *15*, 2514.

(23) White, R. J.; Yoshizawa, N.; Antonietti, M.; Titirici, M. M. *Green Chem.* **2011**, *13*, 2428.

(24) (a) Olson, D. H.; Kokotailo, G. T.; Lawton, S. L.; Meier, W. M. *J. Phys. Chem.* **1981**, *85*, 2238. (b) Treacy, M. M. J.; Higgins, J. B. *Collection of Simulated XRD Powder Patterns for Zeolites*, 5th ed.; Elsevier: Dordrecht, 2007. (c) Kokotailo, G. T.; Lawton, S. L.; Olson, D. H.; Meier, W. M. *Nature* **1978**, *272*, 437. (d) van Koningsveld, H.; Jansen, J. C.; van Bekkum, H. *Zeolites* **1994**, *10*, 235.

(25) (a) Chal, R.; Geradin, C.; Bulut, M.; van Donk, S. *ChemCatChem* **2011**, *3*, 67. (b) Perego, C.; Millini, R. *Chem. Soc. Rev.* **2013**, *42*, 3956.

(26) (a) Cheng, Y. T.; Jae, J.; Shi, J.; Fan, W.; Huber, G. W. *Angew. Chem., Int. Ed.* **2012**, *51*, 1387. (b) Zhao, C.; Lercher, J. A. *Angew. Chem., Int. Ed.* **2012**, *51*, 5935. (c) Li, B.; Sun, B.; Qian, X.; Li, W.; Wu, Z.; Sun, Z.; Qiao, M.; Duke, M.; Zhao, D. *J. Am. Chem. Soc.* **2013**, *135*, 1181.